Scanning Microscopy Vol. 12, No. 2, 1998 (Pages 329-342) 0891-7035/98$5.00+.25
Scanning Microscopy International, Chicago (AMF O'Hare), IL 60666 USA

THE DIAMETER OF DUPLEX AND QUADRUPLEX DNA MEASURED BY SCANNING PROBE MICROSCOPY

J. Vesenka[1]*, T. Marsh[2], E. Henderson[3] and C. Vellandi[1]

[1]Physics Department, California State University, Fresno, CA.
[2]Biology Department, University of Wisconsin, Green Bay, WI.
[3]Zoology and Genetics Department, Iowa State University, Ames, IA.

(Received for publication May 12, 1996 and in revised form October 28, 1996)

Abstract

A review of scanning probe microscopy characterization of duplex DNA morphology bound to mica is presented, including a discussion of numerous proposed contrast mechanisms. The various contrast mechanisms are reexamined in the light of a recently developed form of quadruplex DNA [19]. A discussion of possible morphological changes in duplex DNA and an interesting consequence (e.g., DNA sequencing) is presented.

Key Words: Scanning probe microscopy, atomic force microscopy, low current scanning tunneling microscopy, duplex DNA, quadruplex DNA, G-wire DNA, DNA morphology.

*Address for correspondence:
James Vesenka
Physics Department
California State Univ., Fresno
2345 E. San Ramon MS #37
Fresno, CA 93740-0037

Telephone number: (209) 278-7244
FAX number: (209) 278-7741
E-mail: jamesv@csufresno.edu

Introduction

Plasmid DNA adsorbed onto mica is a model system for investigating the morphology of DNA bound to silicates by two common forms of scanning probe microscopy (SPM), atomic force microscopy (AFM) and low current scanning tunneling microscopy (LCSTM). A fundamental question that has yet to be resolved is the morphology of DNA adsorbed to the silicate substrates. A consistent observation among the many SPM examinations of DNA on mica is the disparity between helix diameter determined by SPM and by classical crystallographic methods. X-ray diffraction studies indicate the common B-form of DNA to be a double stranded helix about 2.0 nm in diameter [24]. However, numerous papers examining naked DNA on mica employing AFM [5, 16] and LCSTM [7], indicate the average height of DNA to be 1 nm or less and the average width to be no less than 3 nm, and usually much wider.

The discrepancy in lateral SPM width measurements of DNA has been attributed in large part to broadening of the image by the finite probe geometry and sample motion. Algorithms have been developed to correct for the probe geometry artifacts to obtain more accurate representations of the sample topography [13, 18, 33]. These improvements tend to be minor for small cylindrically-shaped molecules, such as DNA, since the majority of raw AFM image is comprised of lost information that cannot be completely restored [35]. Less invasive imaging techniques such as "tapping" mode and dynamic force imaging [1, 9, 39] have improved our ability to correct for sample distortions due to lateral forces.

The discrepancy in vertical SPM height measurements of DNA have been more difficult to rationalize. Recent low force tapping mode measurements of DNA height in air (0.79 ± 0.05 nm [8]) and in buffer (0.43 ± 0.08 nm [2]) have reported even smaller dimensions than earlier publications. This is a noteworthy result because it suggests reductions of DNA height dimensions of up to 75% compared to crystallographic data. Only in an exceptional, recent development, involving high resolution studies of densely packed DNA, imaged in contact mode AFM in buffer, has the nearly 2.0 nm diameter helix been obtained after the mica

substrate was modified with cationic lipid bilayers [20]. All these observations are combined into one consistent model in which the treated substrate is proposed to be the source of morphological changes seen in the DNA.

Materials and Methods

Quadruplex DNA [19] and pBR322 DNA (Sigma, St. Loius, MO) were mixed together at a concentration of 50 ng/μl in a buffer consisting of 10 mM Tris (pH 7.8), 1 mM EDTA and 1 mM $MgCl_2$. The sample was allowed to sit on parafilm for 5 minutes at room temperature and adsorbed onto freshly cleaved mica (Ted Pella Inc., Redding, CA), immediately rinsed with 1 ml deionized water, dried in a stream of dry nitrogen and allowed to stabilize in a 37°C oven before imaging. The sample was imaged with both electron beam deposited tip on silicon cantilevers [12] and standard silicon Nanoprobes using a Nanoscope E controller (Digital Instruments, Santa Barbara, CA) in contact mode in dry air and under propanol.

Results and Discussion

Some of the proposed mechanisms to explain the discrepancy in helix diameter of DNA on mica are controllable. In AFM, these observations include: compression due to loading force [4, 38] (Fig. 1), height reduction due to residual buffer salt burial [31] (Fig. 2), and vertical height contrast changes due to cantilever buckling, tip contamination and humidity [26, 27] (Fig. 3). In practice, these contrast mechanisms can be controlled by imaging with low forces, with clean tips, using careful sample spreads and imaging under low humidity. Early in the development of imaging DNA in propanol [8], the low heights obtained of DNA were thought to be partially the result of the dehydration of the DNA in alcohol as the DNA transforms from the B to A conformations. Recently, Hansma and co-workers have developed techniques for imaging under more physiologically relevant buffers employing low probe force tapping AFM [9, 10] (Fig. 4) but without significant improvement in the vertical dimensions of DNA. Lyubchenko and co-workers have suggested that SPM probe-fluid-mica adhesion complex play an important role in DNA height measurements [14, 16]. These, too, can be user controlled, and the height response as a function of substrate has been systematically examined [2]. Systematic studies involving tip chemistry-DNA interactions have been hampered by the invasive nature of tip doping, a process that invariably reduces resolution due to the finite thickness of the dopant (electron beam deposited tips not withstanding).

The disparity in DNA helical diameter is not limited to AFM. An average of 1 nm height was obtained using low current scanning tunneling microscopy, with the reduced DNA diameter being attributed to low sample conductivity [7] (Fig. 5). SPM is routinely capable of 0.1 nm vertical resolution and there are several types of standards that can be used to accurately calibrate the height response [32, 36] so the abnormal dimensions of DNA imaged by SPM is unlikely to be a calibration error. Thundat and co-workers have shown some incidences of stretched DNA [28]. Under these conditions, the height of the stretched DNA is about half the relaxed DNA (Fig. 6). No one has been able to explain conclusively the difference between crystallography and the cumulative scanning probe microscopy results.

There is a natural curiosity as to why this result is obtained so often via different SPM imaging modes. One possibility is that the height discrepancy may actually represent a different morphology of DNA bound to cationic modified silicates. This idea stems from an observation that Marsh *et al*. [19] noted while examining a novel form of quadruplex DNA (G-quartet DNA or "G-wires") co-adsorbed with the well characterized duplex DNA standard. The data suggested that the reduced helical diameter of duplex DNA, observed in tapping mode AFM images, might represent a change in duplex DNA morphology because it measured about 0.7 ± 0.2 nm tall in air and 0.5 ± 0.2 nm in propanol, while the co-adsorbed G-wires measured an average of 2.2 ± 0.2 nm tall in air *and* propanol (Fig. 7). The height dimension of the G-wires were in good agreement with NMR (nuclear magnetic resonance) models (2.4 nm diameter) of G-quartet DNA [19, 22]. In essence, the G-wires, co-adsorbed on the same mica substrate as duplex DNA, acted as a calibration standard from which it was determined that duplex DNA had *uncharacteristic* dimensions, suggesting that the duplex DNA might be flattened or "pinned" against the mica substrate.

Cationic treatment of mica is necessary to adequately bind DNA to the surface for the purpose of SPM imaging [25, 30]. Duplex DNA is thought to adsorb onto the mica surface via cationic bridges (Fig. 8) through the phosphate backbone. If the strength of these bonds are sufficient, pinning of the DNA might cause the flattened DNA to be partially unwound [19] (Fig. 9). The two to three hydrogen bonds in a duplex DNA base pair contribute 2 to 3 kcal/mole each while base stacking adds another 4 to 15 kcal/mole stability to the helix, depending on the base order [24]. A high estimate for the energy that supports the DNA helix between to sets of duplex bases is about 50 kcal/mole. In comparison, G-quartet DNA has a proposed box-like structure that is stabilized by 8 hydrogen bonds/quartet, twice as many base stacking interactions as duplex DNA, plus ionic interactions from quartet pairs surrounding a caged cation [19]. The energy stored between two G-4 rings is somewhere between 100-200 kcal/mole. Therefore, cationic bonds, having an energy of about 75-100 kcal/mole,

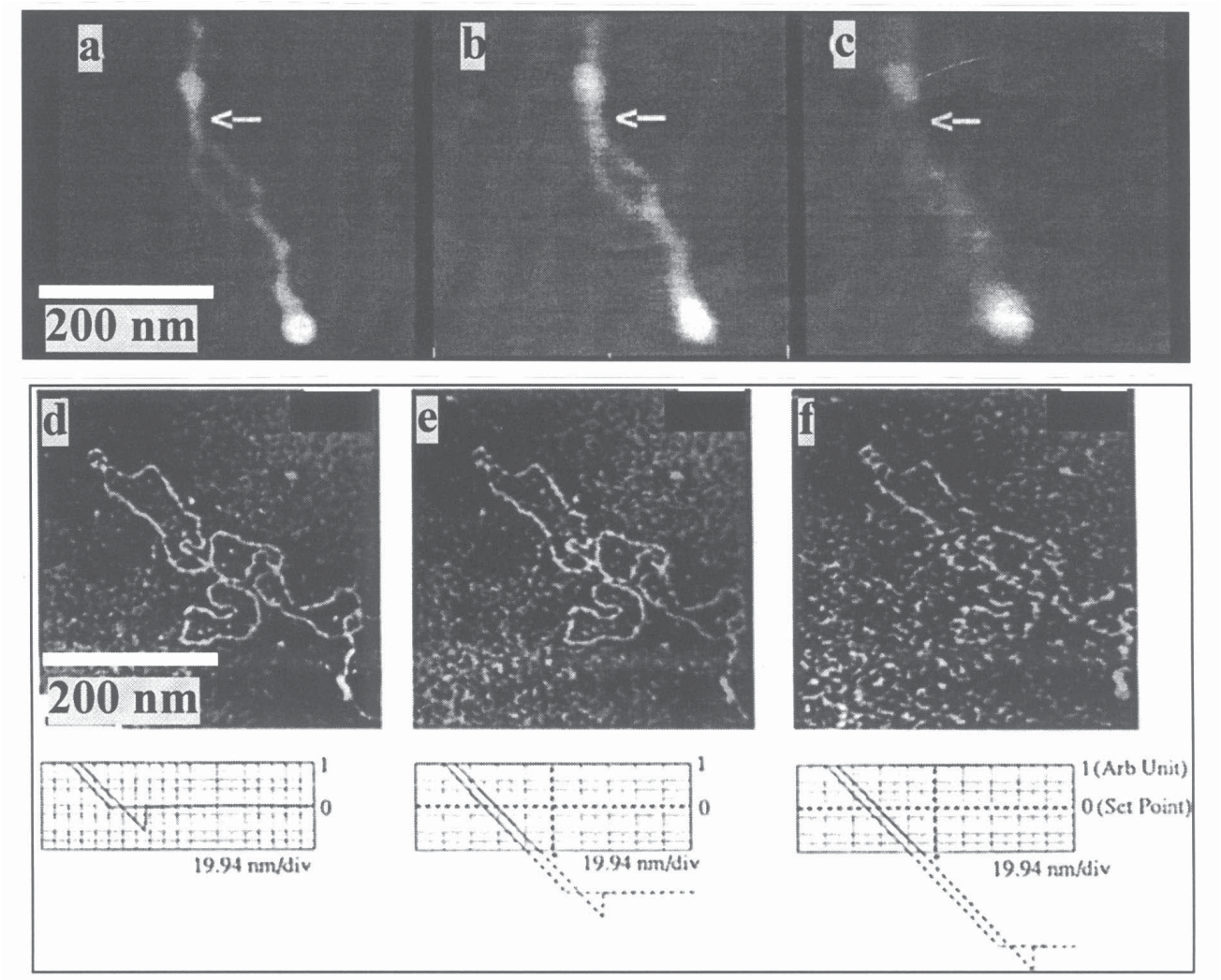

Figure 1. (**a-c**) A series of images illustrating the effect on a plasmid molecule of progressively higher loading forces all images were obtained at 45% relative humidity. (**a**) Loading force of 20 nN, even after repeated scans, height of arrowed region was 1.01 nm and width is 21 nm. (**b**) Loading force of 110 nN, height of arrowed region is 0.62 nm and width is 29 nm. (**c**) Loading force is 170 nN, height is 0.49 nm and width is 47 nm. (**d-f**) Three images of the same DNA molecule under probe forces of 2 (**d**), 9 (**e**) and 12 (**f**) nN, as shown by the force curves below. For (**e**) and (**f**), dashed lines were drawn to indicate the relative levels of the probe forces, because they were out of the range of the display. The horizontal dashed line for (**e**) and (**f**) were positioned according to a linear extrapolation of the set point voltage calibration. The resolution remained approximately constant. But in (**f**), the molecule appeared damaged in many places. Scanning speed for these three images was 4.73 Hz. Humidity was 38%. With permission from references [4] and [38].

might be energetically favorable to tug at the phosphate backbone of duplex DNA enough to partially unwind a duplex helix over a short interval. Eventually the strain, and subsequent stored energy, is so large that helical turn is evident, but not at regular 3.4 nm intervals. However, cationic bonds do not have the energy required to unwind G-quartet DNA which would support the evidence of ability to image quadruplex DNA close to independently verified dimensions.

Stable imaging of DNA was afforded by multivalent cationic or aminopropyltriethoxy silane (APTES) treatment of mica substrates [15]. Greater positive charge density, e.g., by the addition of nickel to the imaging buffer on mica seems to improve reliable imaging under physiologically relevant fluid environments [10]. Routine imaging of the major groove over vast stretches of sample has been

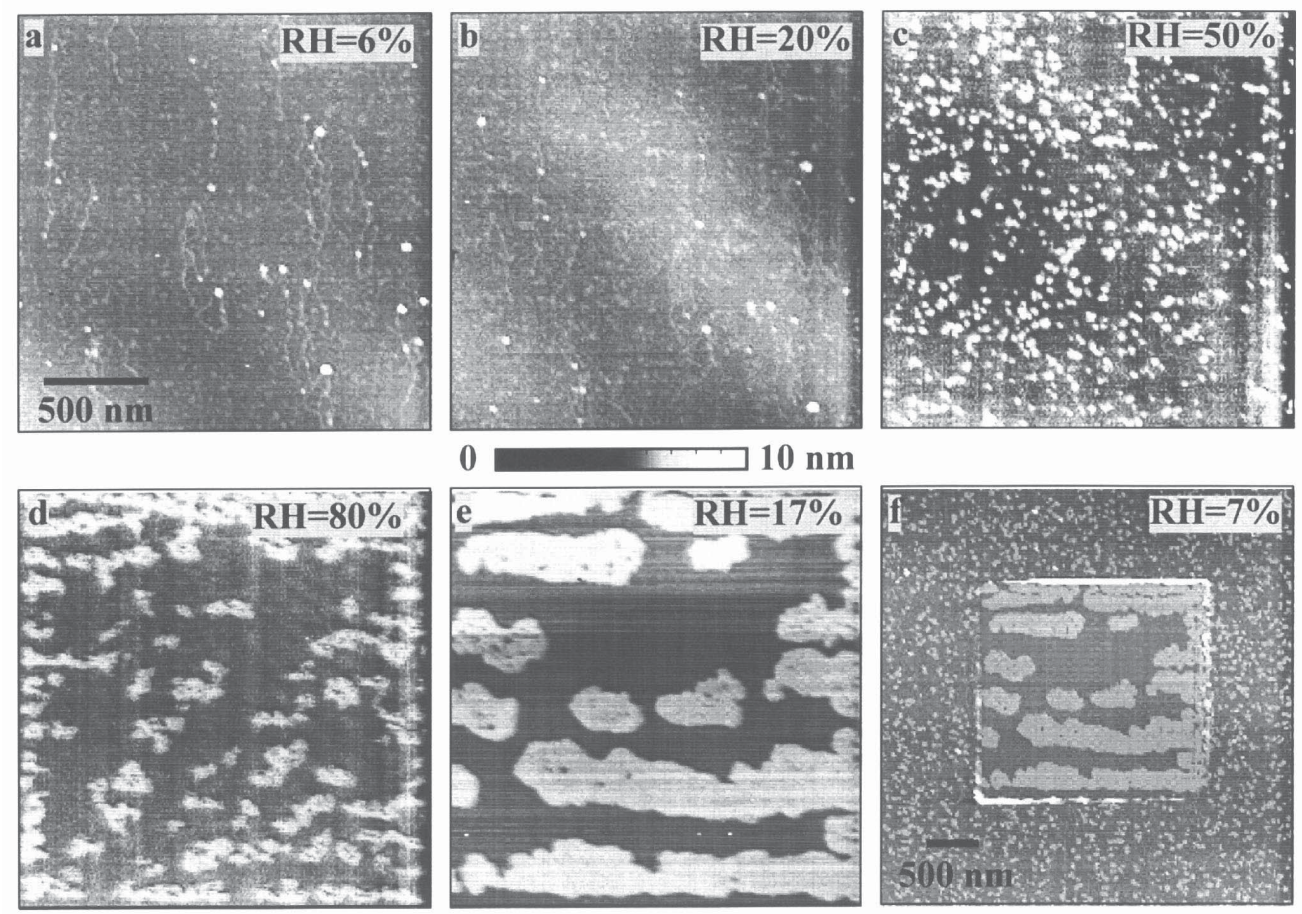

Figure 2. Six images of gold-labeled DNA at different humidity levels. Images (**a-e**) are of the same 2 μm area. Image (**f**) is a 4 μm scan, encompassing the previous scan area, imaged after restoring the humidity to 7%. The repulsive imaging force was maintained at 3 nN for all humidity levels. Note the disappearance of the DNA when the residual salts begin to aggregate under the influence of surface diffusion and the motion of the scanning tip [31].

achieved with densely packed DNA samples on lipid-treated mica [20]. It is reasonable to expect that the packed DNA adds lateral stability to the shear forces generated by an AFM tip in contact mode, enabling the tip to feel the major groove. Thundat has also seen a tendency for spiral packaging of the DNA and attributes this result to charge segregation as the DNA binds to mica [28] (Fig. 10). This may explain the extraordinary high resolution images by Mou *et al*. [20] of packed DNA imaged on cationic lipid bilayers on the surface of mica (Fig. 11).

In Figure 12 both low (a) and high (b) magnification images of a loop of duplex plasmid DNA (pUC119) imaged under propanol. Though there is some tip artifact evident in Figure 12b, which is common for high resolution images, there is also evidence of an average spacing between raised features (arrowed structures) in each loop of about 10.4 ± 1.0 nm. Interestingly, this distance equals three 3.4 nm repeats in the helical repeat structure of native duplex DNA, also seen by Hansma *et al*. [10]. The discrete distances made in this observation could support the proposed pinning model in that **portions** of the DNA helix may be relaxed due to strong interactions between the cationically treated mica and phosphate backbone. According to the analysis of Bustamante and Keller [3] the ability to distinguish between two raised features of similar height separated by distance d with a valley depth of Δz and tip radius of curvature R_c is:

$$d = 2\sqrt{2 R_c \Delta z} \quad (1)$$

In propanol, the height between the pinned DNA and candidate helical twists (arrowed structures) is about 0.3 nm, a typical radius of curvature is 10 nm such that the smallest lateral distance to be resolved is 4.8 nm. This is in agreement with the observed width of the DNA in Figure 12 of about 5

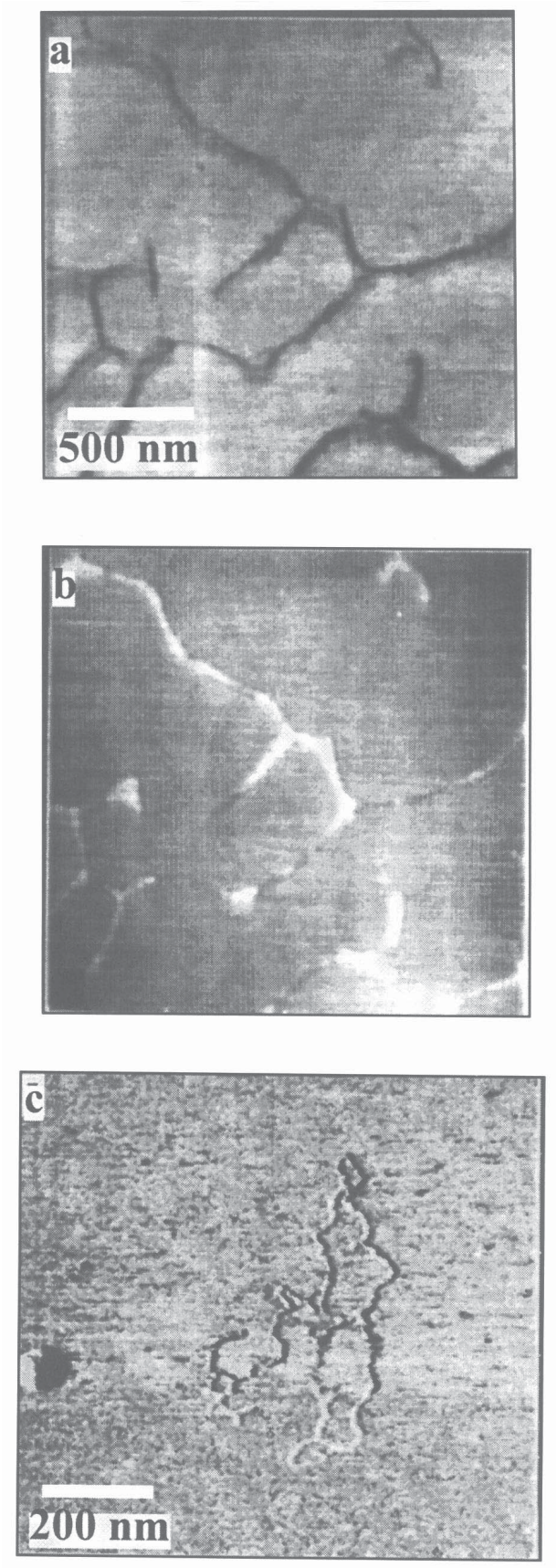

Figure 3. Humidity-dependent positive and negative contrast of AFM images of linear DNA (concentration 3 μg/ml). Black (low) to white (high) corresponds to 5.2 nm. (**a**) 2 μm x 2 μm on mica taken in 60% humidity. The DNA strands show negative contrast. (**b**) Same area of the sample in dry nitrogen ambient. The DNA strands show positive contrast. (**c**) Deflection image of DNA obtained at very low humidity. The change in contrast is very likely due to tip contamination from salt deposit (middle left-hand-edge) during upward scan. Reprinted with permission from references [26] and [27].

nm, an alternative form used to describe lateral resolution [32, 36]. This suggests that the average 10.4 nm spacing may reflect some kind of optimized energy configuration between the DNA and treated mica and leads to the intriguing suggestion that the DNA may be partially unwound.

One of the immediate consequences of flattening due to partial unwinding of duplex DNA would be access to the base pairs within the DNA helix, making partial sequencing of the DNA possible. No high resolution internal DNA structure has been observed within pinned DNA by the AFM. This might be the result of tip-sample chemistry which is complicated by the presence of residual cations. Many of the first attempts to image bases were made on single stranded DNA. However, single stranded DNA tends to base pair with itself, "clumping" the DNA and making it impossible to observe individual bases [10]. Duplex DNA can be made to lie in straight lines on mica [23] potentially facilitating sequencing. A reliable experimental procedure that could unwind the helix of duplex DNA and open up access to the bases might allow determination of the base sequence of the DNA strand, one of the early but unfulfilled promises of SPM technology.

Future Research

DNA and RNA are routinely exposed to silicate surfaces for numerous purposes, including oligonucleotide synthesis [11], determination of the helical period [21], and as a substrate for imaging chromosomes [6, 34]. DNA strongly adsorbs non-covalently onto a variety of silicate substrates (e.g., glass, silicon, or mica). Due to DNA loss by non-covalent adsorption onto silicate surfaces, glassware is treated or scrupulously avoided in special biochemical assays and when small samples of DNA are being examined [17]. As medical diagnostics use more solid state devices (e.g., silicon chips as molecular substrates), understanding the behavior and properties of DNA on silica based surfaces will become critical.

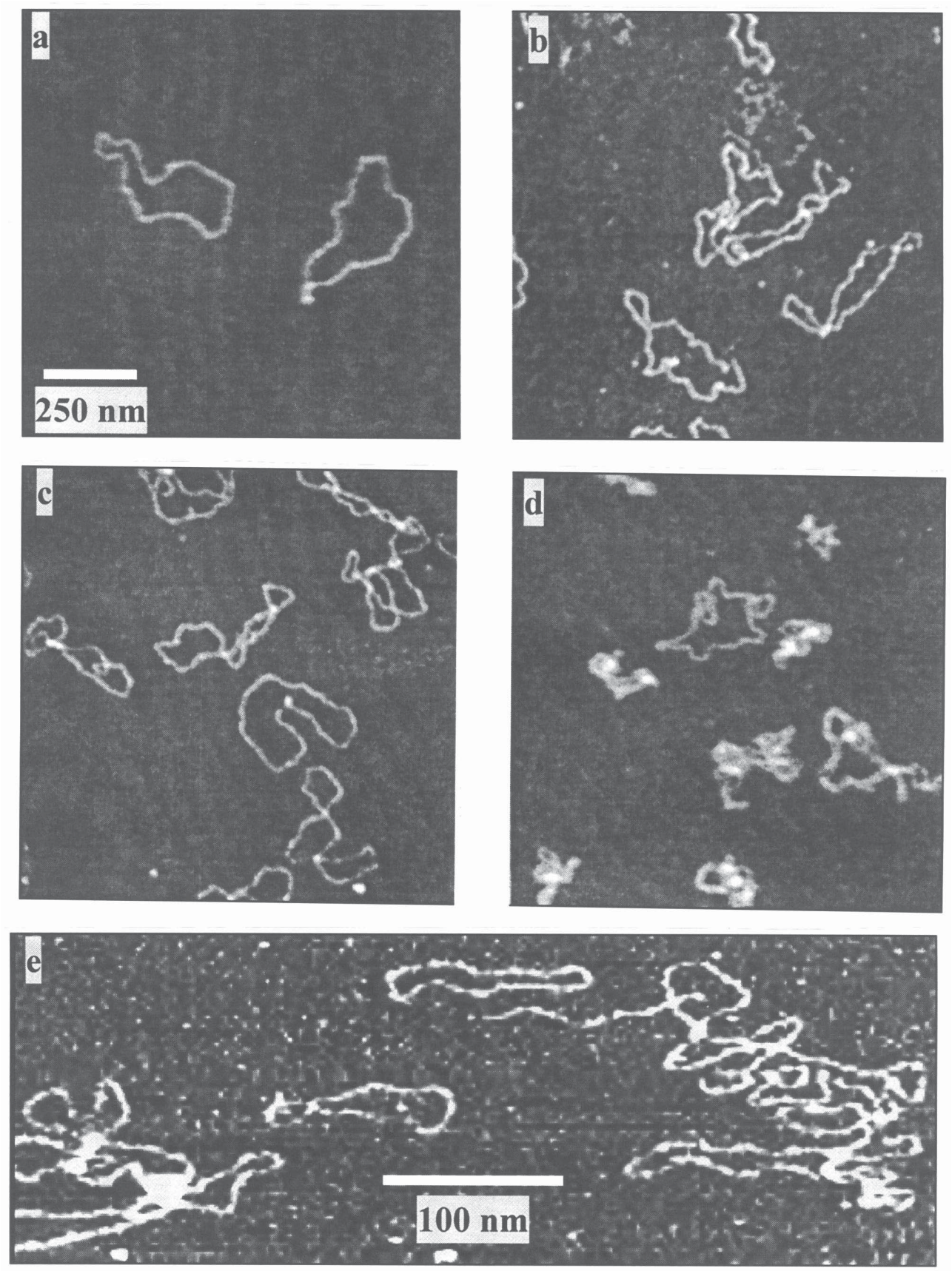
a
250 nm
b
c
d
e
100 nm

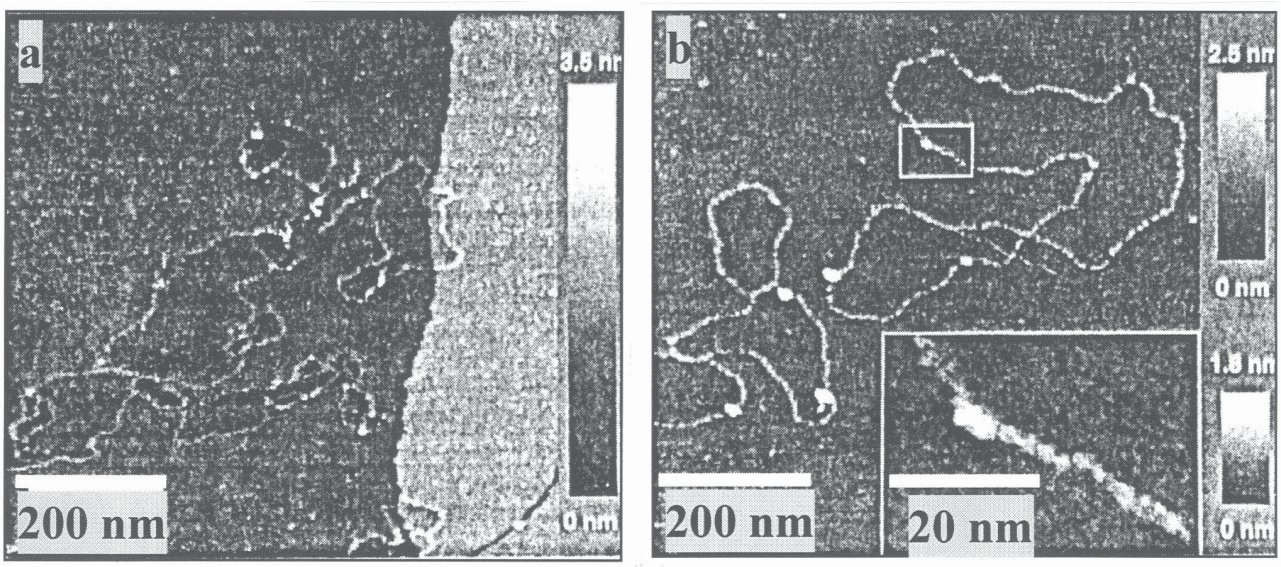

Figure 5. Plasmid DNA (pUC18) adsorbed to mica imaged by STM in humid air. (**a**) The 1 nm step at the right side corresponds to the thickness of one mica layer. The dark line at the bottom right represents a crack in the mica. Imaging conditions: tunneling current, 0.25 pA; sample bias -2.5 V: RH, 66%. (**b**) The box in the overview marks the area displaced in the inset. This inset is a cutout of a zoomed-in image taken immediately after the overview. Imaging conditions: tunneling current, 0.5 pA: sample bias, -7 V; RH, 65%. Reprinted with permission from reference [7].

Figure 4 (*on facing page*). Comparison of DNA under different conditions on mica and AP-mica: (**a**) DNA in water on bare mica, (**b**) DNA in water on AP-mica, (**c**) DNA in HEPES-Mg on bare mica, and (**d**) DNA in HEPES-Mg on AP-mica. (**e**) Plasmid DNA in TE buffer (20 mM Tris-HCl, pH 7.6, 1 mM EDTA). All images were taken in tapping mode with the vertical scale of 5 nm from black to white. Analysis of images taken over smaller areas gives 2.8 ± 0.8 nm for the DNA width and 1.7 ± 0.37 nm for the height. Figures (**a**) through (**d**) reprinted with permission from reference [2]. Figure (**e**) courtesy of Yuri Lyubchenko.

Future efforts in our lab will employ image reconstruction analysis to detect subtle changes in the conformation of DNA on the mica surface. Assuming that normal and lateral probe forces deform the DNA helix to some extent, a small amount of broadening of the width of DNA may be anticipated at the expense of DNA height. However, DNA that has been unwound and pinned flat to mica through cationic bridges between the substrate and phosphate backbone should have a width smaller than that of a probe-induced deformation of the DNA helix. In either case, the DNA width will be broadened further by the finite geometry of the SPM probe apex. The difference in deformed and pinned cross-sectional areas can be estimated from recent sensitive area measuring techniques involving probe and sample reconstruction [35]. Employing the reconstruction models of Vesenka and co-workers, a difference of up to 2.0 nm^2 is expected, well above the ± 0.5 nm^2 sensitivity of their technique. G-wires and colloidal gold particles will be co-adsorbed onto the surface as control samples and to characterize the probe geometry. The cross-sectional area of duplex DNA plasmid and G-wires will be measured as a function of normal and shear loading forces.

Acknowledgments

The authors would like to acknowledge the helpful discussions with Drs. Helen Hansma, Yuri Lyubchenko, Zhifeng Shao and Thomas Thundat. This research was supported through funding from the Research Corporation, the California State University Fresno (CSUF) Research Foundation and the CSUF Associated Students Educational Research Program.

References

[1] Anselmetti D, Lüthi R, Meyer E, Richmond R, Dreier M, Frommer JE, Güntherodt H-J (1994) Attractive-mode imaging of biological materials with dynamic force microscopy. Nanotechnology **5**, 87-94.

[2] Bezanilla M, Manne S, Laney DE, Lyubchenko YL, Hansma H (1995) Adsorption of DNA to Mica, silylated mica, and minerals: Characterization by atomic force

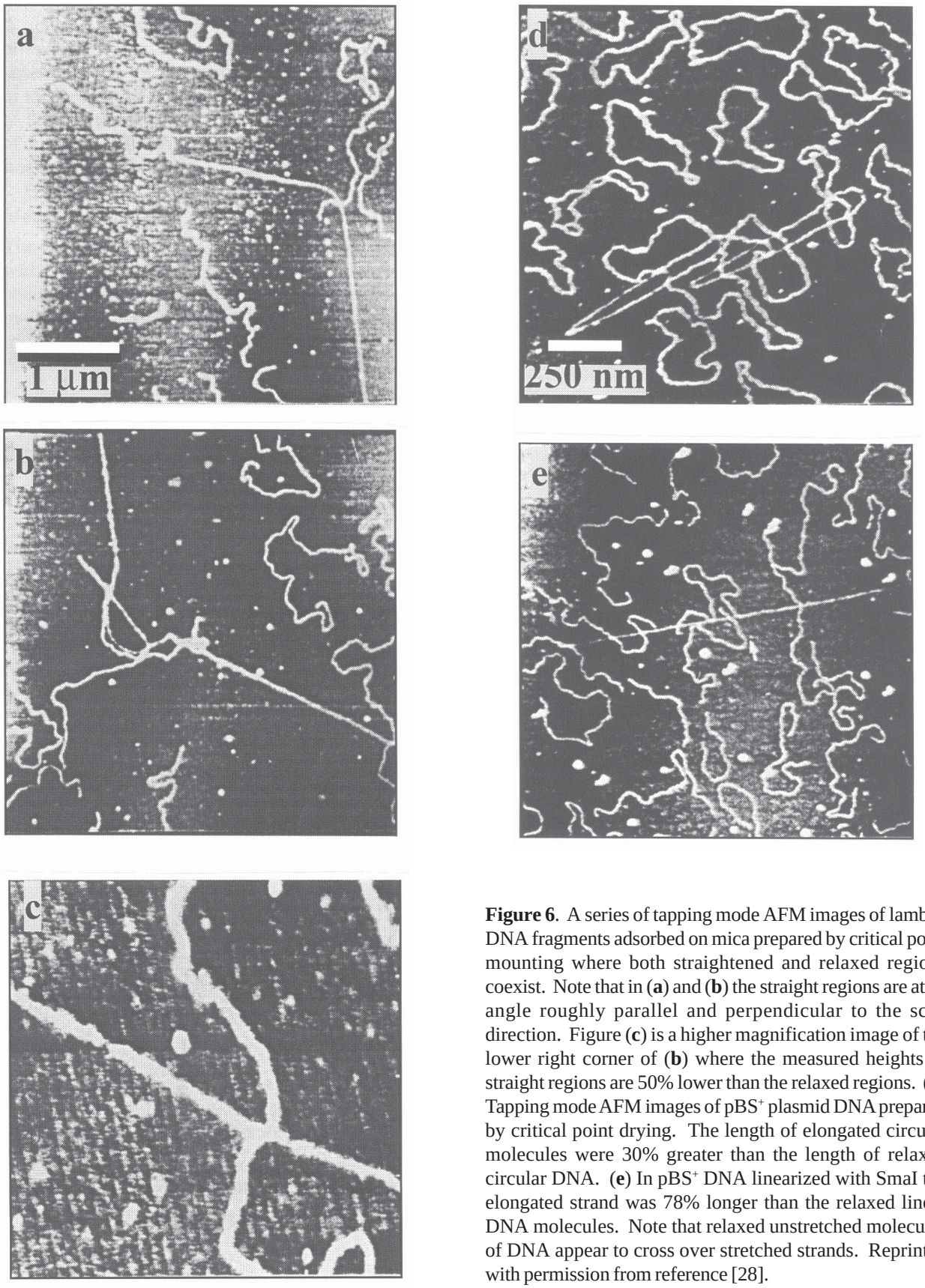

Figure 6. A series of tapping mode AFM images of lambda DNA fragments adsorbed on mica prepared by critical point mounting where both straightened and relaxed regions coexist. Note that in (**a**) and (**b**) the straight regions are at an angle roughly parallel and perpendicular to the scan direction. Figure (**c**) is a higher magnification image of the lower right corner of (**b**) where the measured heights of straight regions are 50% lower than the relaxed regions. (**d**) Tapping mode AFM images of pBS^+ plasmid DNA prepared by critical point drying. The length of elongated circular molecules were 30% greater than the length of relaxed circular DNA. (**e**) In pBS^+ DNA linearized with SmaI the elongated strand was 78% longer than the relaxed linear DNA molecules. Note that relaxed unstretched molecules of DNA appear to cross over stretched strands. Reprinted with permission from reference [28].

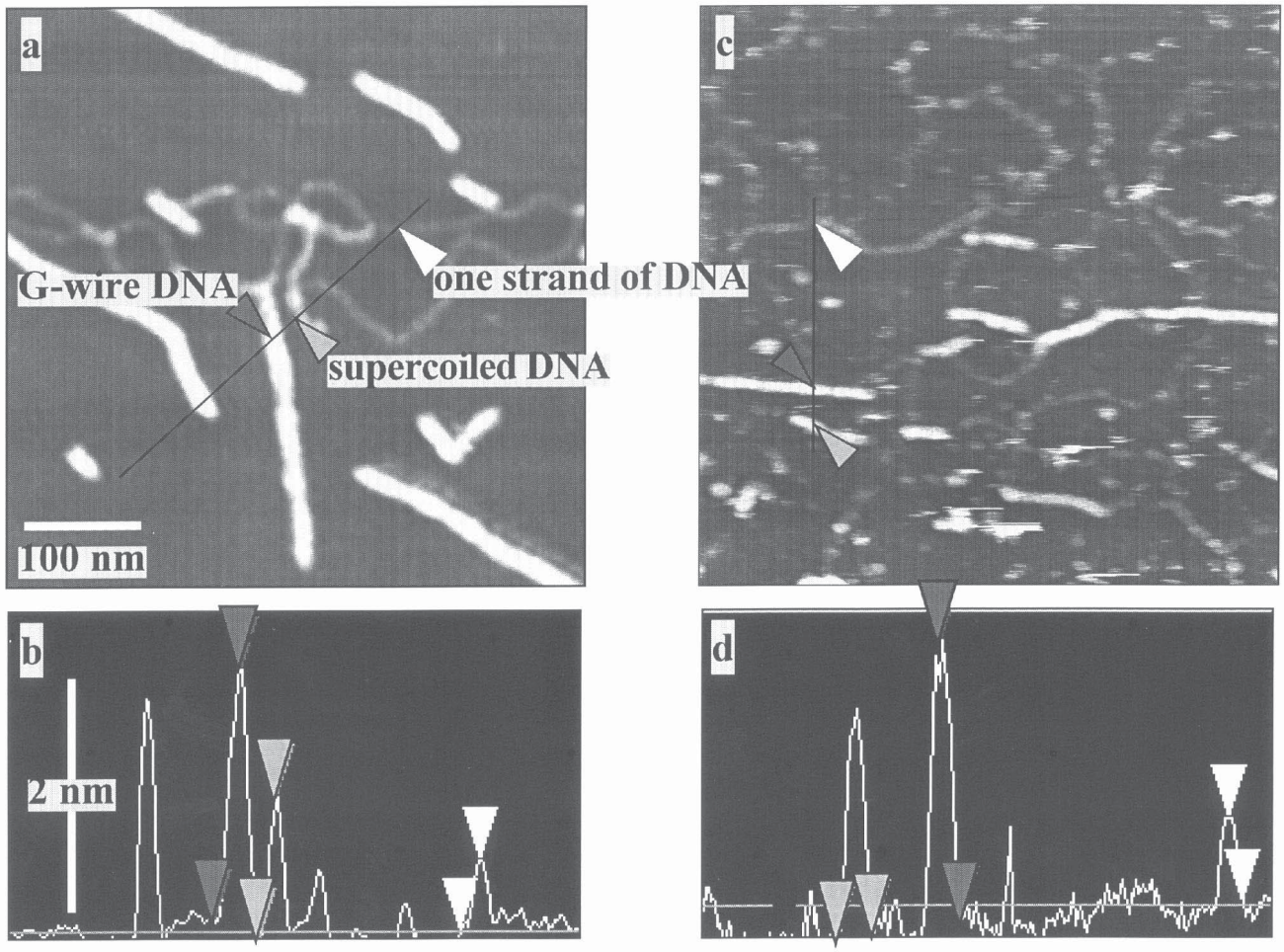

Figure 7. (**a**) Duplex and G-wires coadsorbed on mica with cross section (**b**) imaged in air. Note that the height of the duplex DNA is about half that of the G-wires (dark arrows) where the DNA is **supercoiled** (middle arrows) and almost one quarter of the diameter of the G-wires for relaxed duplex DNA (white arrows). The same mixture was imaged under propanol (**c**), and the cross section (**d**) indicates that the G-wires maintain an average of 2.2 nm diameter, whereas the duplex DNA typically exhibits a further reduction in height. Also note the vast improvement in lateral resolution of both duplex and G-wire when imaging in propanol. Vertical height scale is 10 nm.

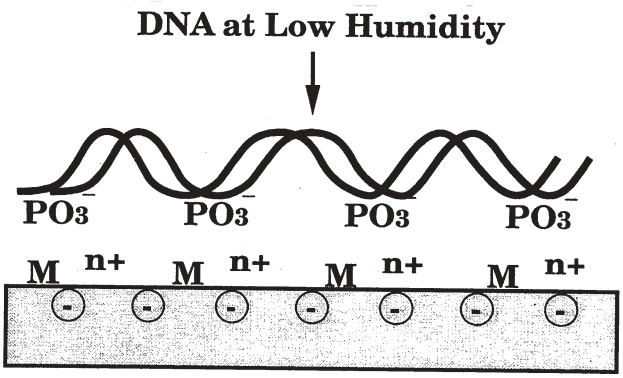

Figure 8 (*at left*). Electronegatively charged phosphate groups from the DNA backbone are stabilized on mica substrate via positively charged cation species.

microscopy. Langmuir **11**, 655-659.

[3] Bustamante C, Keller D (1996) Scanning force microscopy in biology. Physics Today **48**, 32-38.

[4] Bustamante C, Vesenka J, Tang CL, Rees W, Guthold M, Keller R (1992) Circular DNA molecules imaged in air by scanning force microscopy. Biochemistry **31**, 22-26.

[5] Bustamante C, Keller D, Yang G (1993) Scanning force microscopy of nucleic acids and nucleoprotein assemblies. Curr. Op. Struct. Biol. **4**, 363-372.

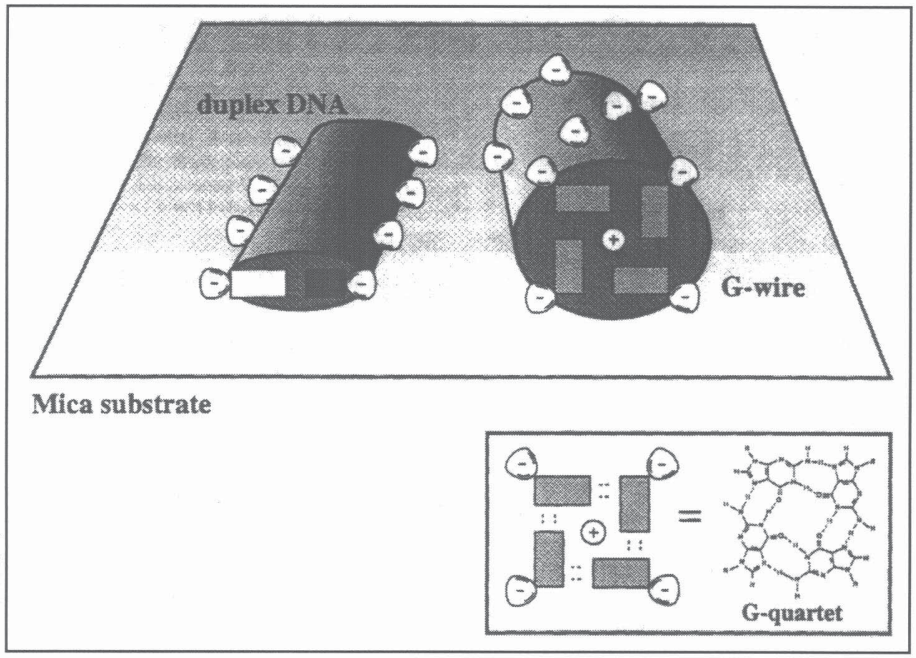

Figure 9. Model of differen-tial stability of duplex DNA and quadruplex DNA during imaging by AFM. The height of plasmid DNA is significantly diminished compared to the height of the G-wire. A possible explanation is that an uncoiling of the double helix occurs as the DNA molecule is adsorbed to the substrate and dried [37]. The quadruple helical G-wires have a coordinated cation that provides additional stability to the structure, thereby providing resistance to conformation change upon surface binding. The height of the G-wires correlates with the stabilizing capacity of the coordinated cation ($K^+ > Na^+ > Mg^{2+}$) [29]. With permission from reference [19].

[6] Fritzsche W, Vesenka J, Henderson E (1995) Scanning force microscopy of chromatin. Scanning Microsc. **9**, 729-739.

[7] Guckenberger R, Heim M, Cevc G, Knapp HF, Wiegräbe W, Hillebrand A (1994) Scanning tunneling microscopy of insulators and biological specimens based on lateral conductivity of ultrathin water films. Science **266**, 1538-1540.

[8] Hansma H, Vesenka J, Kelderman G, Morrett H, Sinsheimer R, Elings V, Bustamante C, Hansma PK (1992) Reproducible imaging and dissection of plasmid DNA under liquid with the atomic force microscope. Science **256**, 1180-1184.

[9] Hansma PK, Cleveland JP, Radmacher M, Walters DA, Hillner PE, Bezanilla M, Fritz M, Vie D, Hansma HG, Prater CB, Massie J, Fukunaga L, Gurley J, Elings V (1994) Tapping mode atomic force microscopy in liquids. Appl. Phys. Lett. **64**, 1738-1740.

[10] Hansma HG, Laney DE, Bezanilla M, Sinsheimer RL, Hansma PK (1995) Applications of atomic force microscopy of DNA. Biophys. J. **68**, 1672-1677.

[11] Kaplan B, Itakura K (1987) DNA synthesis on solid support and automation. In: Synthesis and Applications of DNA and RNA. Narang SA (ed.)., Academic Press, Inc., Orlando, FL. pp. 9-45.

[12] Keller D, Chih-Chung C (1992) Imaging steep, high structure by scanning force microscopy with electron beam deposited tips. Surf. Sci. **268**, 333-339.

[13] Keller DJ, Franke FS (1993) Envelope reconstruction of scanning probe microscope images. Surf. Sci. **294**, 409-414.

[14] Lyubchenko YL, Oden PI, Lampner D, Lindsay SM, Dunker KA (1993) Atomic force microscopy of DNA and bacteriophage in air, water and propanol: The role of adhesion forces. Nucleic Acids Res. **21**, 1117-1123.

[15] Lyubchenko Y, Shlyakhtenko L, Harrington R, Oden P, Lindsay S (1993) Atomic force microscopy of long DNA: Imaging in air and under water. Proc. Natl. Acad. Sci. USA **90,** 2137-2139.

[16] Lyubchenko YL, Jacobs BL, Lindsay SM, Stasiak A (1995) Atomic force microscopy of nucleoprotein complexes. Scanning Microsc. **9**, 705-727.

[17] Maniatis T, Fritsch EF, Sambrook J (1982) In: Molecular Cloning, a Laboratory Manual. Cold Spring Harbor Laboratory, Cold Spring Harbor, NY. p. 437.

[18] Markiewicz P, Goh MC (1994) Atomic force microscopy probe tip visualization and improvement of images using a simple deconvolution procedure. Langmuir **10**, 5-7.

[19] Marsh T, Vesenka J, Henderson E (1995) A new DNA nanostructure imaged by scanning probe microscopy. Nucleic Acids Res. **23**, 696-700.

[20] Mou J, Czajkowsky DM, Zhang Y, Shao Z (1995) High resolution atomic force microscopy of DNA: The pitch of the double helix. FEBS Lett. **371**, 279-282.

[21] Rhodes D, Klug A (1980) Helical periodicity of DNA determined by enzyme digestion. Nature **286**, 573-579.

[22] Sen D, Gilbert W (1992) Novel DNA superstructures formed by telomere-like oligomers. Biochemistry

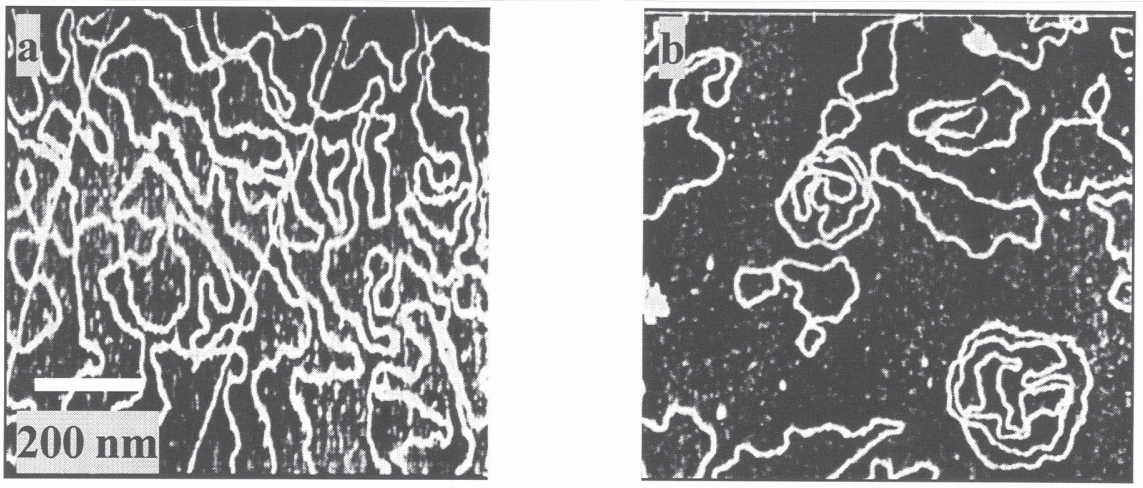

Figure 10. AFM image of (**a**) fragments of lambda DNA and (**b**) pBS^+ showing possible electrostatic repulsion between the strands. The relaxed DNA strands do not interact and remain separate from one another. In the lambda DNA preparation (**a**) some of the DNA strands appear to be straightened. Note that unstretched relaxed DNA fragments freely cross the anomalous DNA. With permission from reference [28].

31, 65-70.

[23] Shaiu WL, Larson DD, Vesenka J, Henderson E (1993) Atomic force microscopy of oriented linear DNA molecules labeled with 5 nm gold spheres. Nucleic Acids Res. **21**, 99-103.

[24] Sinden RR (1994) DNA Structure and Function. Academic Press, San Diego, CA. pp. 12-14, 23-25.

[25] Thundat T, Allison DP, Warmack RJ, Brown GM, Jacobson KB, Schrick JJ, Ferrell TL (1992) Atomic force microscopy of DNA on mica and chemically modified mica. Scanning Microsc. **6**, 911-918.

[26] Thundat T, Allison DP, Warmack RJ, Ferrell TL (1992) Imaging isolated strands of DNA molecules by atomic force microscopy. Ultramicroscopy **42-44**, 1101-1106.

[27] Thundat T, Warmack RJ, Allison DP, Bottomley LA, Lourenco AJ, Ferrell TL (1992) Atomic force microscopy of deoxyribonucleic acid strands adsorbed on mica: The effect of humidity on apparent width and image contrast. J. Vac. Sci. Technol. A **10**, 630-636.

[28] Thundat T, Allison DP, Warmack RJ (1995) Stretched DNA structures observed with atomic force microscopy. Nucleic Acids Res. **22**, 4224-4228.

[29] Venczel EA, Sen D (1993) Parallel and antiparallel G-DNA structures from a complex telomeric sequence. Biochemistry **32**, 65-70.

[30] Vesenka J, Guthold M, Tang CL, Keller D, Delaine E, Bustamante C (1992) Substrate preparation for reliable imaging of DNA molecules with the scanning force microscope. Ultramicroscopy **42-44**, 1243-1249.

[31] Vesenka J, Manne S, Yang G, Bustamante CJ, Henderson E (1993) Humidity effects on atomic force microscopy of gold-labeled DNA on mica. Scanning Microsc. **7**, 781-788.

[32] Vesenka J, Manne S, Giberson R, Marsh T, Henderson E (1993) Colloidal gold particles as an incompressible atomic force microscope imaging standard for assessing the compressibility of biomolecules. Biophys. J. **65**, 992-997.

[33] Vesenka J, Miller R, Henderson E (1994) Three-dimensional probe reconstruction for atomic force microscopy. Rev. Sci. Instrum. **65**, 2249-2251.

[34] Vesenka J, Mosher C, Schaus S, Ambrosio L, Henderson E (1995) Combining optical and atomic force microscopy for life sciences research. Biotechniques **19**, 240-253.

[35] Vesenka J, Marsh T, Miller R, Henderson E (1996) Atomic force microscopy image reconstruction of G-wire DNA. J. Vac. Sci. Tech. B. **14**, 1413-1417.

[36] Xu S, Arsndorf MF (1994) Calibration of the scanning (atomic) force microscope with gold particles. J. Microsc. **173**, 199-210.

[37] Yagil G, Sussman JL (1986) Effect of substrate on DNA topology. EMBO J. **5**, 1719-1725.

[38] Yang J, Shao Z (1993) Effect of probe force on the resolution of atomic force microscopy of DNA. Ultramicroscopy **50**, 157-170.

[39] Zhong Q, Inniss D, Kjoller K, Elings VB (1993) Fractured polymer/silica fiber surface studied by tapping mode atomic force microscopy. Surf. Sci. Lett. **290**, L688-L692.

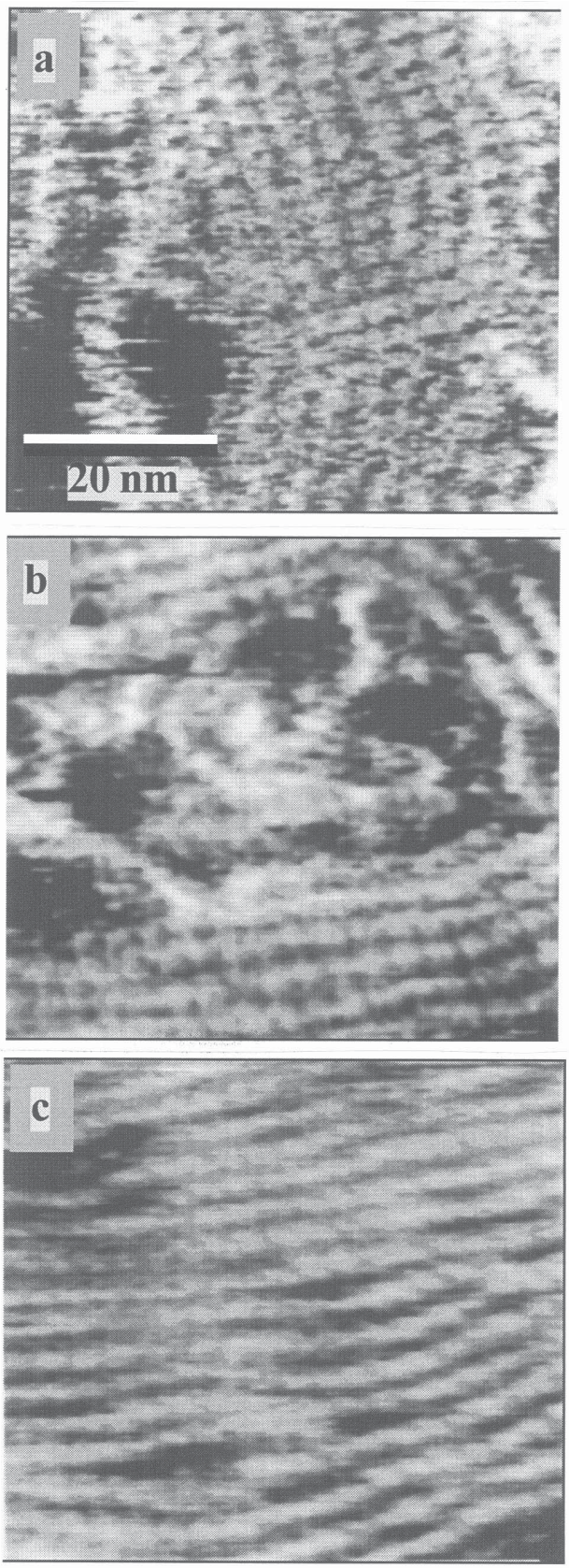

Figure 11. The right handedness of the double helix is also resolved by the AFM. These results show the excellent stability of these samples and the reproducibility of AFM. (**a**) pBR322 (4.36 kb). (**b**) pBR325 (6 kb). (**c**) *Hae*III restriction fragments of øX174. Occasionally, even the minor grooves were recognizable (see b). It is also seen that the handedness is better resolved when the DNA strand is parallel with the fast scan direction (see c). This is because the instrumental drift is more noticeable in the slow scan direction. With permission from reference [20].

Discussion with Reviewers

Y.L. Lyubchenko: Partial unwinding of DNA caused by interaction with the substrate should lead to elongation of the molecules. Was this effect observed by the authors?
Authors: This question is an important test of the pinning model. The authors are currently pursuing experiments to measure the change in contour lengths due to DNA intercalators, molecules that will relax the helix of the DNA, leading to an increase of contour length. Side-by-side comparisons of contour length from samples of DNA on mica that are not intercalated might help establish a meaningful baseline difference. Unfortunately, a calculation of the amount of contour length increase based on intercalation of relaxed DNA results in only a small change of overall length, about 10%, currently within the statistical noise of contour length measurements. It is expected that the pinning model would result in even smaller changes in contour length measurements. It is hoped that more accurate measurements of the counter length that account for the artificial broadening of the tip shape might improve these statistics and enable a meaningful comparison.

H.G. Hansma: How reproducible is the 10 nm lump spacing for different samples and different tips? From how many samples and tips were these data taken? In our experience, I thought the lump spacing was typically 8-12 nm, i.e., more variable than reported here, but we have not analyzed it in detail. Based on the quality of the image in Figure 12, it seems like a lot of high quality image gathering needs to precede image reconstruction.
Authors: These results were reproducible from two different samples taken with two different tips each. The authors have seen this behavior over many years, like Hansma, but never sat down to quantify the observations before. The result of an "average" 10 nm lump spacing is exactly that, an average taken over 100 points from several different plasmids. The authors carefully include the caveat under the Figure caption, also in the text, that tip geometry can not be ruled out as the source of this repeated affect. It

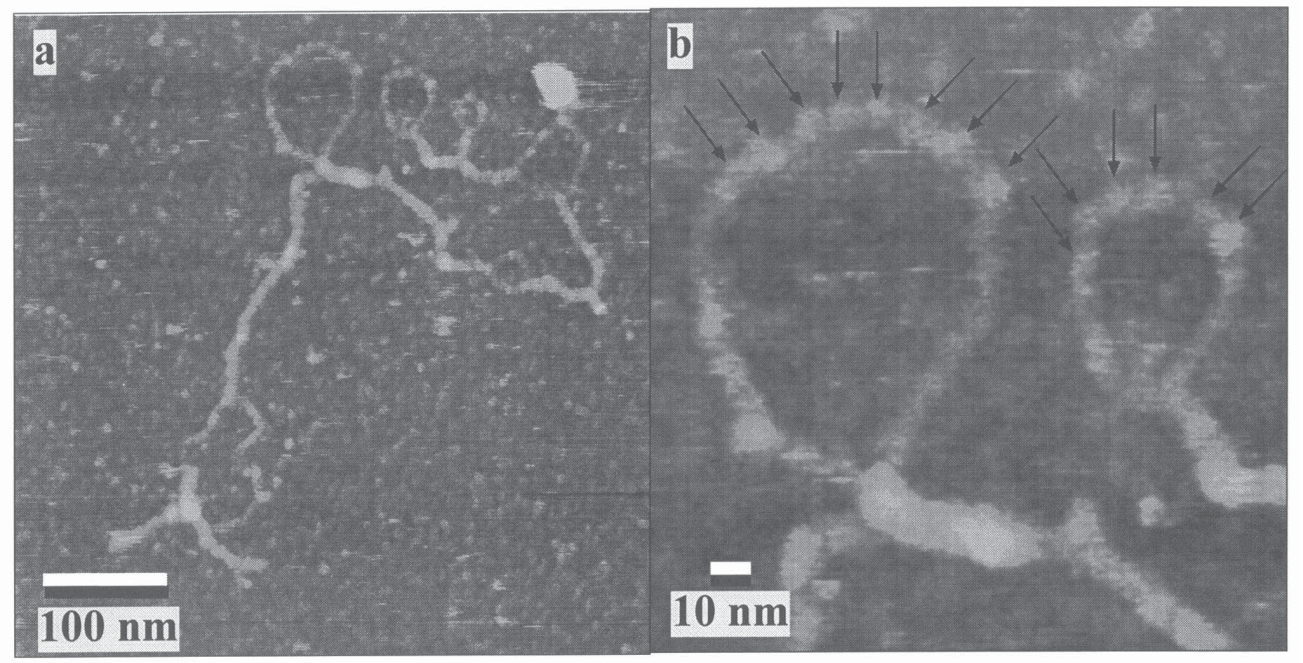

Figure 12. Low (**a**) and high (**b**) magnification images of a loop in double stranded DNA (pUC119) imaged under propanol. The average spacing between raised features (arrowed in (**b**)) in each loop is about 10.4 ± 1.0 nm. This distance equals exactly three 3.4 nm repeats in the helical structure of native duplex DNA, in agreement with the model proposed in the text that portions of the DNA helix are partially relaxed due to strong interactions between the cationically treated mica and phosphate backbone. Based on the ability to distinguish between individual raised features with a valley of 0.3 nm height separating them, and a tip radius of curvature of 10 nm, the closest resolved features could be as close as 4.8 nm apart (see text, **Results and Discussion**, for details). This is in agreement with the width the DNA and suggests that the average 10.4 nm spacing may reflect some kind of optimized energy configuration between the DNA and treated mica.

---

is here that image reconstruction is potentially most valuable. However, the authors still lack intermittent contact imaging (e.g., DI's Tapping® Mode) and are unable to keep calibrations particles secured on mica in propanol long enough to obtain a useful tip calibration. No image reconstruction was carried out on these samples for that reason, and no mention that this technique was used was made in the text. However, the image reconstruction procedure, once a satisfactory field of gold particles has been found to act as a calibration standard, is a very robust process. High quality data is needed only in the sense that a sharper tip allows for more of the sample to be "seen." A blunt tip yields no more useful data with image reconstruction that it does without it. The bottom line is that image reconstruction is a partial fix when tips are reasonably sharp. The field of biological AFM still needs sharp, robust tips.